Proceedings of GT2005
ASME Turbo Expo 2005: Power for Land, Sea and Air
June 6-9, 2005, Reno-Tahoe, Nevada, USA

GT2005-68917

LAMINAR FLAME SPEEDS OF SYNTHETIC GAS FUEL MIXTURES

J. Natarajan, S. Nandula, T. Lieuwen, and J. Seitzman
School of Aerospace Engineering
Georgia Institute of Technology
Atlanta, GA 30332-0150

ABSTRACT

Laminar flame speeds of H_2/CO/CO_2 mixtures have been measured over a range of fuel compositions, lean equivalence ratios, and reactant preheat temperature (up to 700 K). The measurements are compared to numerical flame speed predictions based on two reaction mechanisms: GRI Mech 3.0 and a H_2/CO mechanism. For undiluted and nonpreheated mixtures, the current results agree with previous data and the numerical calculations over most of the range tested. The measured flame speeds increase as the H_2 content of the fuel rises and for higher equivalence ratios. The most significant difference between the measurements and models is for high CO content fuel with the H_2/CO mechanism, and the high H_2 content fuel at the leanest conditions with the GRI mechanism. For CO_2 diluted fuels, measured flame speeds decrease as predicted. However, agreement between the measurements and predictions worsens with increasing CO_2 dilution. Deviations as large as 40% are observed at lean equivalence ratios and 20% CO_2 levels. For reactant preheat temperatures below ~400K, the measured flame speeds generally match the calculated flame speeds within 10%. At higher preheat temperatures, however, the discrepancy between the measurements and the calculations increases, reaching levels of ~30% at 700 K. The measured temperature dependence is closer to the predictions from GRI Mech 3.0 than from the H_2/CO mechanism.

[*Keywords:* Syngas, Laminar flame speed, CO_2 dilution, reactant preheat]

INTRODUCTION

Technologies such as integrated gasification combined cycle (IGCC) plants enable combustion of coal, biomass, and other solid or liquid fuels while still maintaining high conversion efficiencies and low pollution emissions. Synthetic gas (syngas) fuels derived from coal are particularly promising in this regard. Syngas fuels are typically composed primarily of H_2 and CO, and may also contain smaller amounts of CH_4, N_2, CO_2, H_2O, and other higher order hydrocarbons.[1,2] The specific composition depends upon the fuel source and processing technique. This substantial variability in composition, and also heating value, provides one of the largest barriers towards their usage. Understanding the impact of this variability on combustor performance or emissions requires an understanding of the fundamental combustion properties of these mixtures.

Therefore, the objective of this study is to improve understanding of the laminar flame speed (S_L) characteristics of syngas fuels. Laminar flame speed is an important parameter of a combustible mixture as it contains fundamental information regarding reactivity, diffusivity, and exothermicity. The value of the flame speed has important impacts upon the propensity of a flame to flashback and blowoff, and also controls other key combustion characteristics, such as the flame's spatial distribution.

Several prior studies have initiated measurements of the flame speeds of syngas-type mixtures. Laminar burning velocities of syngas mixtures have been measured with Mach Hebra nozzle burners[3] and with Bunsen burners.[4] Laminar flame speeds of CO/H_2 mixtures have also been measured with spherically expanding flames[5] and flat flames.[6] However, most of these flame speed measurements are in stoichiometric and fuel-rich mixtures; many low emissions gas-turbine approach require lean premixed combustion. There is also substantial scatter in the reported data that could not be explained just by experimental uncertainties (see review by Andrews and Bradley[7]).

Stretch corrected measurements of S_L in H_2/CO counter-flow flames[8] and spherically expanding flames[9-12] have been obtained more recently and are in fair agreement with each other. However, they cover a limited range of equivalence ratios, relative H_2/CO concentrations, and, most significantly, are restricted to room temperature reactants. Furthermore, most of the measurements are for atmospheric pressures; an

exception is the work of Hassan *et al.*[12], who have measured flame speeds at pressures up to 5 atm. Similarly, limited measurements are available for fuels with CO_2 dilution. Some measurements and computational studies of CH_4 diluted with CO_2 (to simulate landfill gas) have been reported.[13,14] Little data on H_2/CO mixtures diluted with CO_2 is available.

Clearly, there is a need to extend the range of available flame speed data for syngas mixtures, particularly at realistic engine conditions. Obtaining such measurements is the objective of our study. We have initiated an extensive study of syngas mixture flame speeds with compositions reflecting those that may be encountered in fuel-flexible combustors. This paper describes the initial results of the study; laminar flame speeds of H_2/CO mixtures over a wide range of fuel composition (i.e., H_2:CO ratio), equivalence ratio, CO_2 dilution (up to 20%), and reactant preheating (unburned temperatures up to 700 K) are reported.

BACKGROUND

The propagation and stability properties of syngas (H_2/CO) mixtures are not well documented, and performance characteristics of these mixtures cannot be simply inferred from knowledge of the global performance of the constituents. To begin with, CO and H_2 have significantly different transport properties (e.g., Lewis numbers) and flame speeds. Next, CO chemistry, which releases slightly more heat than the same amount of H_2 by mass, is strongly coupled to H_2 oxidation,[9,12] for example through the reaction $CO+OH \rightarrow CO_2+H$, which dominates CO conversion under many conditions.

Furthermore, the main branching reaction for H_2 as well as wet-CO[15] combustion is $H+O_2 \rightarrow O+OH$. Hence, addition of H_2 to CO/air flames results in increased laminar flame speeds of the mixture. The added H radicals from H_2 lead to increased branching and accelerate the rate of CO oxidation. The relative increase in S_L is more pronounced at lower H_2 levels in CO/air systems.[13]

As previously noted, syngas fuels have a large variability not only in the fuel content, but also in the diluents, e.g., the composition of CO_2 can typically range from 1.6-30%.[1] The presence of CO_2 in the fuel will impact the flame in at least three ways, through changes in: 1) mixture specific heat and adiabatic flame temperature, 2) chemical kinetic rates, and 3) radiative heat transfer. First, the molar specific heat of CO_2 is larger than that for the fuels it displaces (CO and H_2). Therefore, the addition of CO_2 will lower the reactant temperatures in the preheat region and the adiabatic flame temperature and, thus, the laminar flame speed. Since CO_2 has a higher molar specific heat than air, it reduces the adiabatic flame temperature and flame speed more than an equal amount of air dilution. Thus the flammability limits and extinction strain rates of the CO_2 diluted mixtures are correspondingly narrower. This point has been emphasized in several studies on the effects of CO_2 dilution on CH_4[13,14,16] and H_2 flames[17].

Second, CO_2 does not act as a passive diluent in the fuel, but interacts kinetically. The kinetic effects of CO_2 dilution are manifested primarily in the main CO oxidation reaction, $CO+OH \rightarrow CO_2+H$. Higher CO_2 levels lead to enhanced back reaction rates and, hence, reduced CO oxidation and enhanced consumption of H atoms. In lean H_2/CO flames, the H atoms are extremely important as they control the main branching ($H+O_2 \rightarrow O+OH$) and termination ($H+O_2+M \rightarrow HO_2+M$) reactions. Since CO_2 dilution alters the H atom concentration, CO_2 can have profound effects on flame propagation and flame speeds of H_2/CO flames. This effect is further pronounced at higher pressures, as the three-body termination reaction dominates, resulting in lower flammability limits on the lean side. Chemical kinetic studies have emphasized this point by comparing the flame speeds of mixtures with CO_2 dilution, and a fictitious chemically inert species with the same specific heat as CO_2, showing that the CO_2 diluted flame speed had lower flame speeds.[16]

The third effect of CO_2 dilution is through enhanced levels of radiation, as CO_2 is a more effective absorber and radiator than oxygen or nitrogen. CO_2 dilution can result in lower flame temperatures and lower laminar flame speeds (compared to air dilution) due to radiative losses from the flame.[14] In a numerical study of these effects in methane flames, Ruan *et al.*[18] reported that the optically thin model loses effectiveness for large CO_2 dilution ratios and lower equivalence ratios. Furthermore, nongray radiation[19] must be considered to predict laminar burning velocity and flammability limits of flames with CO_2 dilution, especially at elevated pressures.

EXPERIMENTAL FACILITY

Figure 1 is a schematic of the experiment used for the laminar flame speed (S_L) measurements. The desired fuel composition is first prepared using a bank of calibrated rotameters, one for each gas. After mixing thoroughly, the fuel is split into two flows: the desired flowrate of fuel passes through another rotameter (calibrated for the particular fuel composition), while the remainder is flared in a diffusion flame. Finally, the required quantity of air is added, and the mixture goes to the burner. This arrangement allows simple control over the equivalence ratio (ϕ) and the average velocity through the burner. All the rotameters are calibrated with a bubble flow meter to $\pm$ 1% accuracy, with fuel flows in the range of 0.1 to 5 slpm.

Various burners are employed; each is a straight cylindrical stainless steel tube, with inner diameters (D) ranging from 4.5 to 18 mm. The length of each tube is at least 50D in order to ensure that the flow is laminar and that the exit velocity profile is fully developed. The burner diameter is chosen to ensure that the flow remains laminar (Reynolds number, $Re_D < 2000$) and that the average velocity is at least five times greater than the estimated laminar flame speed for a given fuel composition. Thus the premixed flame is stabilized on the rim of the burner. The reactants are preheated by electrical resistance tape

wrapped around the burner. Once the desired reactant temperature is achieved (as determined by a type-K thermocouple, TC2, temporarily placed at the burner exit), the surface temperature of the burner is monitored by a second thermocouple, TC1, and held constant by a temperature controller. The mixture temperature at the exit of the burner is radially uniform (3-5 K) across the burner.

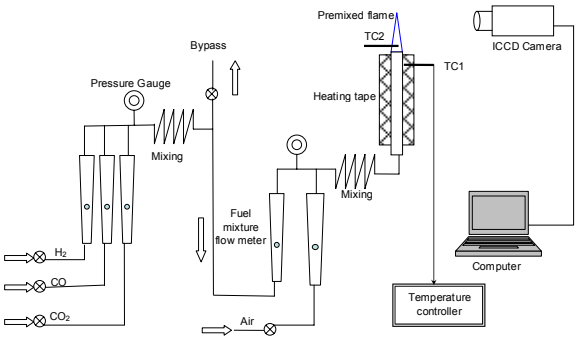

Figure 1. Schematic of the experimental setup (TC=thermocouple). Mixing is achieved through long flow lines.

Digital images of the flame emission are captured with a 12-bit intensified CCD camera (576 × 384 pixels) and a 105 mm, f/4.5 UV camera lens. The camera system is sensitive in the ultraviolet and visible regions (~220-650 nm), and hence is capable of capturing OH^*, CO_2^* and CH^* chemiluminescence from the flame reaction zone. Figure 2 shows a more detailed view of the imaging system, which includes an unusual feature, a horizontal knife edge placed in front of the lens in order to vary the collection solid angle along the flame height.

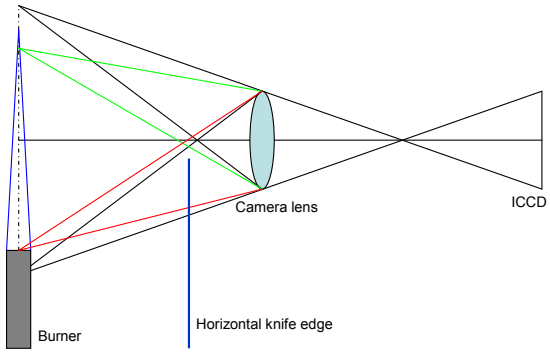

Figure 2. Detailed view of the imaging system with horizontal knife edge.

Figure 3 shows some typical images of the flame radiation. The majority of the flame emission comes from the flame edge, i.e., chemiluminescence from the reaction zone. The less intense region in the central portion of the image is due primarily to chemiluminescence from the front and back edges of the flame. As seen in Figure 3a, the intensity of standard methane flame acquired without the knife edge is relatively constant with height, though slightly higher at the base due to the decrease in integrated flame area in the axial direction. As described below, the flame speed calculation depends on locating the reaction zone. Thus large variations in intensity with height will be problematic. This is evident for high H_2 concentration flames (Figure 3b and d) acquired without the knife edge and 3 ms exposures. For these cases, the H_2 fraction (and thus ϕ) can also decrease along the height of the flame since H_2 has an unusually high diffusivity. This exacerbates the intensity variation with flame height and makes it difficult to determine the flame area.

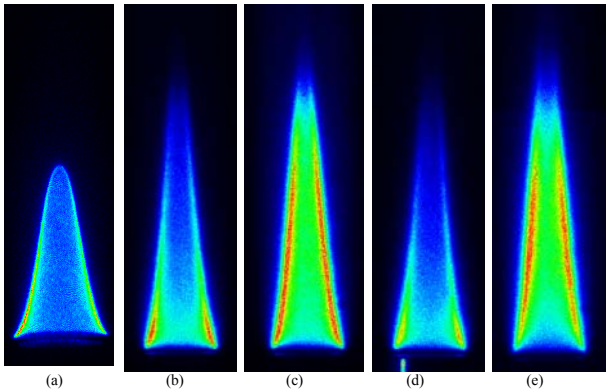

Figure 3. Images of flame emission for various fuels and conditions: (a) CH_4, ϕ=0.77, (b) H_2:CO=95:5, ϕ=0.61 without knife edge, (c) same as (b) but with knife edge, (d) H_2:CO=95:5 and 20% CO_2, ϕ=0.62 without knife edge, (e) same as (d) with knife edge. The color scale is black and dark blue for low intensities, and green, yellow and red for higher intensities.

As indicated in Figure 2, the horizontal knife edge reduces the amount of light coming from the flame base while the amount of light coming from the flame tip remains unchanged. By increasing the exposure time (~25 ms), the tip of the flame is made visible, without saturating the ICCD image of the flame base. The result is seen in Figure 3c and e. The flame tip is clearly visible in these images, and thus the flame area can be calculated more accurately.

FLAME SPEED CALCULATION

Method

The laminar flame speed is defined as the velocity that a plane flame front travels relative to the unburned gas in a direction normal to the flame surface. Though the laminar flame speed is straightforward in definition, in practice it is difficult to measure. Hence some assumptions have to be made in its measurement. A flame stabilized on the rim of a tube burner is conical in shape and not one dimensional. This conical flame is affected by strain and curvature whose effect on local flame speed depends on the effective Lewis number of the mixture. As such, our flame speed measurement is an area weighted average over the entire flame surface. Moreover, this rim stabilized flame is not truly adiabatic because of heat loss to the burner rim (as well as some radiation losses). The heat

loss reduces the flame speed, but the effect should be small and confined primarily to the base of the flame.

In our experiments, the average flame speed is calculated by dividing the volume flow rate of the mixture with the luminous inner cone surface area. It is clear from the definition of the laminar flame speed that the true flame area should be the unburned flame area, just upstream of the preheat zone of the flame. Hence, our calculated flame area should be slightly over predicted, and the flame speed under predicted, by using the luminous inner cone area as the flame area.

To calculate the luminous inner cone area, an edge detection program has been developed using MATLAB. The flame is assumed to be axially symmetric about the axis of the burner; thus we split each flame image in half through the burner axis, as seen in Figure 4a. The edge detection program detects the inner edge of the flame by locating the maximum derivative of the flame intensity along the radius of the flame (Figure 4b). The flame location points are then fit to a fifth degree polynomial (Figure 4c). The flame area is then found using the axisymmetric assumption. The same procedure is repeated for the other half of the flame image, and the change in flame area between these two sections is always less than 1%. The average of the two flame areas was used for the flame speed determination for each image.

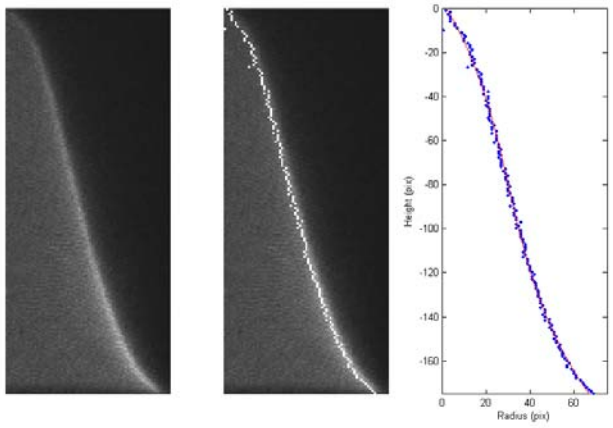

(a) (b) (c)

Figure 4. Flame edge determination: (a) CH_4 flame, ϕ=0.77, (b) edge detected image, (c) 5th degree polynomial fit to flame edge.

For each experimental condition, typically 25 images are recorded and the corresponding flame areas are calculated. Since the flame is not enclosed or isolated from the atmosphere in the present experiment, low velocity flames are affected more by the ambient environment, resulting in greater perturbations in the flame area. The laminar flame speed (S_L) is calculated from

$$S_L = \frac{\dot{Q}}{A}$$

where $\dot{Q}$ is the volume flow rate of the mixture and A is the average flame area from the set of (25) images.

Comparisons with Existing Measurements

Experiments were conducted for various CH_4-air and H_2-CO-air mixtures and compared with previous results from the literature in order to validate the technique. For CH_4-air mixtures, the appropriate burner diameter was chosen to be 18 mm. Figure 5 shows results for CH_4-air flames; the flame speed peaks just rich of stoichiometric. The measured flame speeds are in good agreement with previous results obtained in a premixed, counterflow flame.[20, 21]

The good agreement between the curved jet flame and 1-d counterflow flame can be interpreted as follows. On one hand, it may suggest that the errors in flame speed measurement associated with the current approach are small. It is also possible that the increase in flame speed due to the negatively stretched jet flame (because the fuel is the deficient species and more diffusive) may be offset by the reduction in flame speed due to the over prediction of the flame area (assuming inner luminous cone area as the true unburned flame area). On the rich side, the measured flame speed is slightly, but consistently lower than that determined in the counterflow flame. The flame speed decreases for the negatively stretched jet flame if the deficient species (in the rich side it is air) is less diffusive. Hence, in the rich side, both stretch effect as well as the over prediction in the flame area decrease the flame speed than that of the counter flow methodology.

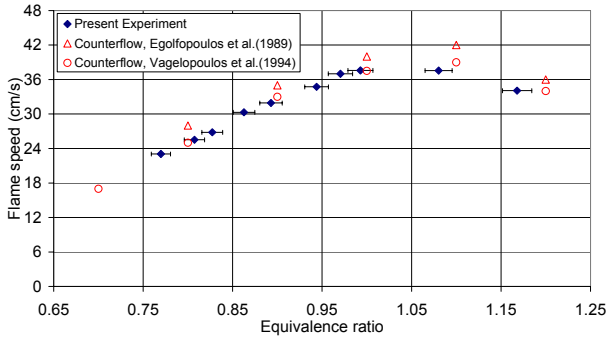

Figure 5. Variation of the measured flame speed for CH_4 with equivalence ratio.

Validation experiments were also conducted for two H_2-CO fuel compositions: 50:50 and 5:95 (Figure 6). The appropriate burner diameters were chosen to be 4.5mm and 13.6mm, respectively. For each of these mixtures, the equivalence ratio was varied from 0.6 to 1. The flame speed increases with equivalence ratio for both the mixtures, and increasing the amount of CO in the fuel decreases the flame speed for a given equivalence ratio. The measured flame speeds are in good agreement with literature values[9] obtained from spherical flames. For example, the reported stoichiometric flame speed for the 50:50 mixture is 115 cm/s, which is very close to the present measurement of 112 cm/s. The 5:95 results are also in close agreement, though with slight (<10%) differences near stoichiometric mixtures. Again these comparisons suggest that the current technique is accurate, though it is possible that the increase in flame speed due to the

negatively stretched flame could be fortuitously offset by the reduction in flame speed due to over prediction of the flame area.

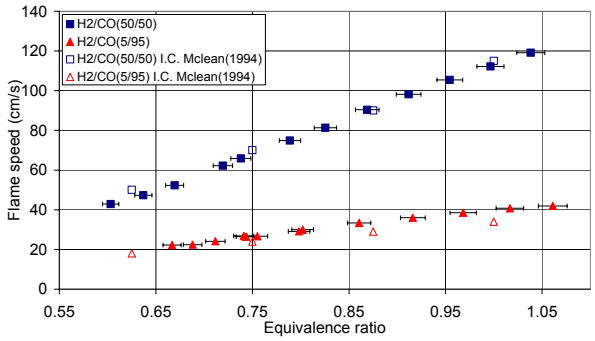

Figure 6. Measured flame speeds for H_2:CO 50:50 and 5:95 fuel compositions.

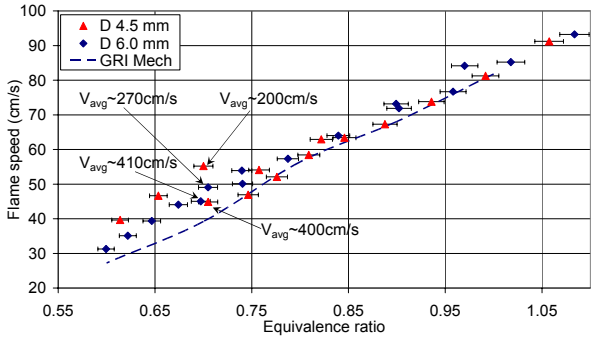

Figure 7. Flame speed measurements for a H_2:CO 50:50 fuel mixture with different burner diameters and average velocities.

MEASUREMENT UNCERTAINTY

The measured laminar flame speed exhibits some dependence on the burner diameter and the average velocity of the mixture. This is mainly due to the fact that the change in burner diameter or average velocity changes strain and curvature of the flame, which in turn changes the flame speed. Experiments were conducted for a 50:50 H_2:CO fuel composition with two different diameters and different average velocities, while maintaining laminar and stable flame conditions (see Figure 7). The average velocity decreases as the equivalence ratio decreases due to the decrease in the flame speed and blowoff gradient. It can be observed that for a given diameter, the increase in average velocity reduces the measured flame speed. For example, the measured flame speed and average velocity at ϕ~0.7 are indicated for both the diameters in Figure 7. It is clear from these values that for a given diameter, increasing the average velocity decreases the measured flame speed. When the average velocity increases, the flame height increases, which increases the straight region of the flame and reduces the curvature affected tip area.

Generally, the negative curvature near the flame tip area increases the flame speed if the fuel is more diffusive and is the deficient species in the mixture, which is true for lean H_2:CO mixtures. Due to this lesser curvature, and thus the reduced tip area dependence at higher average velocity, the flame speed decreases. Hence to reduce the uncertainty in the flame speed measurement due to this curvature and strain effect, all the remaining results were obtained with the highest possible velocity for a given diameter, while maintaining laminar flow and a stable flame.

The determination of flame area and flame speed was also examined for its dependence on which chemiluminescence source (OH^* and broadband CO_2*) is used to define the flame zone. Experiments were conducted with and without an OH^* 308nm bandpass filter for a 50:50 H_2:CO fuel composition with 0% and 20% CO_2 dilution. Figure 8 shows flame images with and without the OH^* filter; except near the flame tip region, there is little difference between the images.

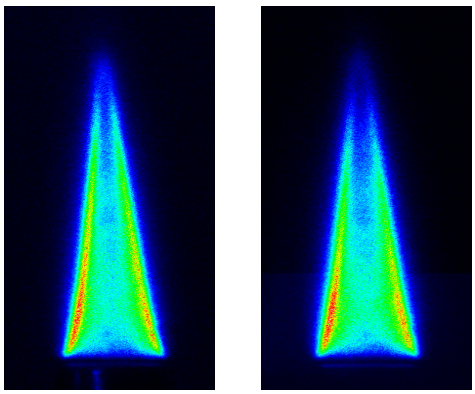

Figure 8. Chemiluminescence images of H_2:CO 50:50 fuel composition for ϕ=0.6 (a) broadband chemiluminescence (b) with 308nm band pass filter (primarily OH^*). The exposure time for the filtered image was increased to offset the reduced transmission.

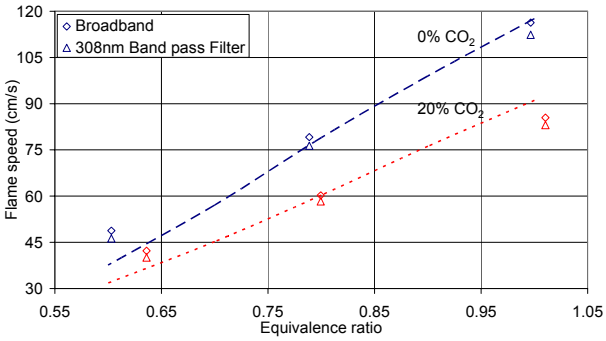

Figure 9. Comparison of the measured flame speed for H_2-50% & CO-50% fuel with and without OH^* filter.

Figure 9 shows the slight difference in measured flame speed for the different radiation sources. The average velocity was the same for both cases at a given equivalence ratio. The discrepancy between the measured flame speeds is less than the discrepancy due to velocity or diameter change. Thus to improve signal-to-noise ratio and reduce experimental times, broadband chemiluminescence was used for the results presented in this work.

RESULTS AND DISCUSSION

One of the prime objectives of the present work is to measure the flame speed for syngas (H_2-CO) compositions with varying levels of CO_2 dilution and preheating under lean conditions. This will allow validation or improvement of the models used to compute syngas flame properties. For this reason, we also compare the results to one-dimensional flame speeds calculated using the Chemkin PREMIX code with two reaction mechanisms, GRI Mech 3.0 and the H_2/CO mechanism of Davis et al.[22] GRI Mech 3.0 is a mechanism that has been tested and validated extensively for methane chemistry. The second mechanism that we chose is a mechanism developed recently for H_2/CO combustion. This mechanism is built on the kinetic model of Mueller et al.[23] with rate parameters and efficiencies that have been revised over the last few years. Three different H_2:CO compositions were examined: 95:5, 50:50 and 5:95, in order to cover a broad range of compositions.

Effect of CO_2 Dilution

A 5:95 H_2:CO mixture was tested with a burner diameter of 13.6mm. The results without CO_2 dilution were presented previously in Figure 6 and are shown again in Figure 10. The measured flame speeds, as with that of the spherical flame results, are above the computed flame speeds across the equivalence ratio range. The discrepancy, however, is not more than 5% between the measurements and flame speeds computed with GRI Mech. There is a greater discrepancy, however, with the H_2/CO mechanism.

To identify the major cause for the difference between the two predictions, the GRI Mech 3.0 flame speed predictions were recalculated with one change in the mechanism; the rate constant for the reaction CO+OH→CO_2+H was replaced with the expression used by Davis et al.[22] These new computed flame speeds along with the results from the unaltered GRI and Davis mechanisms are shown in Figure 11. The results based on the same CO+OH rate are in good agreement, even though the rest of the kinetic mechanism is different. Clearly, the laminar flame speed predictions for H_2-CO mixtures where CO is the predominant fuel are extremely sensitive to the rate model for CO+OH→CO_2+H. The H_2/CO mechanism of Davis et al. was optimized and validated for flame speeds with the spherical flame results of McLean et al.[9] (as indicated by the excellent agreement seen in Figure 11). Given the scatter in the kinetic rate data[22-23] for the CO+OH→CO_2+H reaction, this rate could be adjusted to fit the current experimental flame speed data. Further experiments and modeling studies are necessary to investigate this issue.

Figure 10 also shows the effect of 10% CO_2 dilution on flame speeds for the 5:95 H_2-CO mixture (i.e., the fuel composition is 4.5% H_2, 85.5% CO and 10% CO_2). Addition of CO_2 decreases the flame speed, primarily because dilution lowers the flame temperature and hence the rate of the CO and H_2 oxidation reactions. It is also possible that the increased thermal radiation from the higher CO_2 levels increases the heat loss from the flame, and reduces the flame temperature and flame speed. Since the effect of radiation is not included in the computations, the good agreement between the measured and computed flame speeds with GRI mechanism suggests radiation is not a large effect under these conditions. It is also possible that the increase in flame speed due to negative stretch of the jet flame, *if it is significant*, is offset by the CO_2 radiation losses, leading to the good agreement. The flame speeds computed with the H_2/CO mechanism are lower than the measurements by ~10%, similar to the undiluted case.

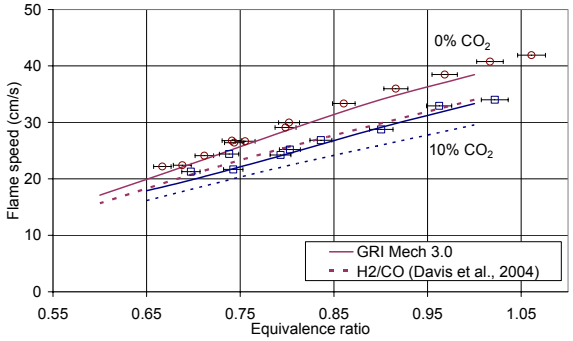

Figure 10. Variation of the flame speed with ϕ for a 5:95 H_2:CO composition with 0 and 10% CO_2 dilution. The curves are results from PREMIX , with GRI-Mech 3.0 and H_2/CO mechanism of Davis et al.[22]

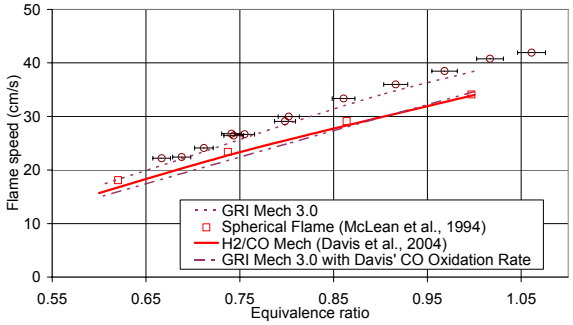

Figure 11. Variation of flame speed with ϕ for a 5:95 H_2:CO mixture. The curves are results from PREMIX, with different reaction mechanisms. Our data and spherical flame data are also shown in the figure.

Figure 12 shows flame speeds for 50:50 H_2:CO fuels with 0-20% CO_2 dilution and a burner diameter of 4.5mm. As the amount of CO_2 increases, the tip of the flame becomes less intense, and hence, the knife edge was used to make the tip clear for accurate flame area calculation, especially for the 20% CO_2 dilution case. For all the CO_2 dilution cases, the flame speeds computed with both mechanisms are nearly the same for this equally weighted H_2/CO composition. The measured flame speeds for the no dilution case agree well to the computed values over the entire equivalence ratio range. As the amount of CO_2 increases, the measured flame speeds decrease as expected and are in reasonably good agreement (within 5%) with the

computed flame speeds for near stoichiometric conditions. The discrepancy between the computed and measured flame speeds increases for leaner mixtures, with the computed flame speed under predicting the measured value by 10-20% for ϕ=0.75-0.6.

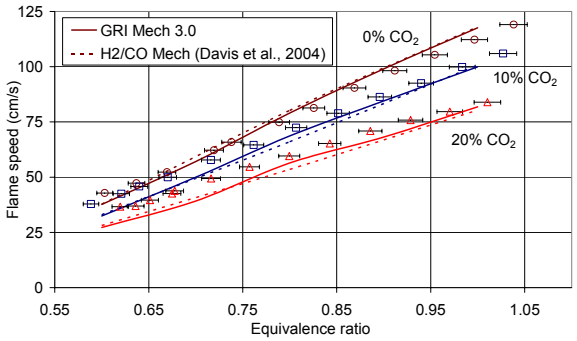

Figure 12. Variation of the flame speed with ϕ for a 50:50 H_2:CO composition with 0, 10%, and 20% CO_2 dilution. The curves are results from PREMIX , with GRI-Mech 3.0 and H_2/CO mechanism of Davis et al.[22]

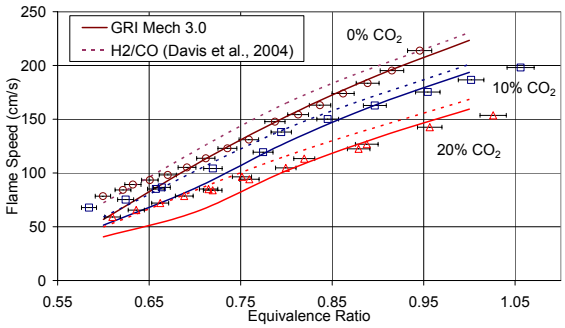

Figure 13. Variation of the flame speed with ϕ for a 95:5 H_2:CO composition with 0, 10%, and 20% CO_2 dilution. The curves are results from PREMIX , with GRI-Mech 3.0 and H_2/CO mechanism of Davis et al.[22]

Figure 13 shows similar results for a 95:5 H_2:CO fuel composition with varying CO_2 dilution and the same 4.5 mm burner diameter. The measured flame speeds for all three CO_2 dilution cases are in good agreement with the computed flame speeds using GRI Mech 3.0 near stoichiometric conditions and the computed flame speeds with the H_2/CO mechanism under very lean conditions. The computed flame speeds are different from the measured values by as much as 30-40%. One possible explanation for these results is that one of the computed flame speeds is correct, but that another effect, e.g., CO_2 radiation, varies with equivalence ratio in a way that produces the measured results. Another possibility is a weakness in both mechanisms. It should be noted here that unlike the 5:95 case, the kinetic rate of CO oxidation has very little affect on the computed flame speeds. Although both these mechanisms have been "validated" for H_2 flames, neither mechanism has been validated previously for H_2 flames with small levels of added CO. These results suggest a need to reassess the chemical mechanisms for syngas mixtures with high H_2 content.

Effect of Preheating

Experiments were carried out for premixed reactant mixtures with fuels composed of 5:95, 50:50, and 95:5 H_2:CO over a range of temperatures from approximately room temperature to 700 K. As the unburned reactant temperature increases, the flame speed and reactant viscosity also increase. The increase in flame speed leads to a need to operate at higher average flow velocities; fortunately, the flow remains laminar due to the corresponding increase in gas viscosity. Hence, the same diameter burners were used for the preheated cases as in the room temperature case.

The influence of preheat temperature for a 5:95 H_2:CO composition is shown in Figure 14. The measured and computed flame speeds are in good agreement up to a preheat temperature of ~400 K over the entire range of ϕ. As the temperature increases further, the discrepancy between the measured and computed flame speeds (both mechanisms) increases, with larger differences near stoichiometric conditions. The computed flame speeds under predict the measured values by as much as 10% for GRI Mech 3.0 and as much as 20% for the H_2/CO mechanism.

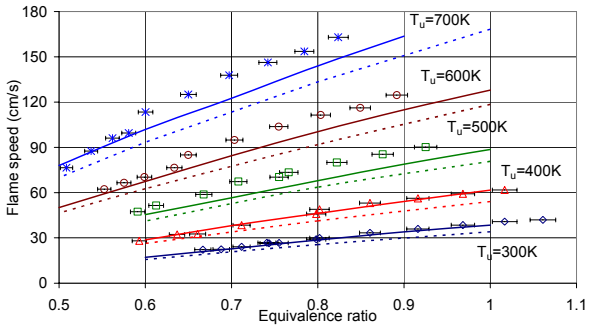

Figure 14. Flame speeds for a 5:95 H_2:CO composition (no dilution) for various preheat temperatures. The curves are results from PREMIX, with GRI-Mech 3.0 (solid lines) and H_2/CO mechanism (dashed lines) of Davis et al.[22]

Similar results for the 50:50 H_2:CO composition are shown in Figure 15. As in the 5:95 case, the computed and measured speeds are in good agreement up to ~400 K. Above this temperature, the discrepancy between the two again increases. Also as before, the discrepancy is larger for the flame speeds computed with the H_2/CO mechanism. The temperature dependence for the 50:50 fuel composition is more clearly seen in Figure 16. The discrepancy between the measured and the computed flame speed increases rapidly above a preheat temperature of 400-450 K. Unlike the 5:95 case, the computed flame speeds under predict the measured values for all equivalence ratios. For example when the fuel-air mixture is preheated to 600 K, the computed flame speeds over predict the measured value by 10-15% with GRI Mech and by 12-17%

with the H_2/CO mechanism. If the unburned temperature increases further, the computed flame speeds are 20-30% above the measured values.

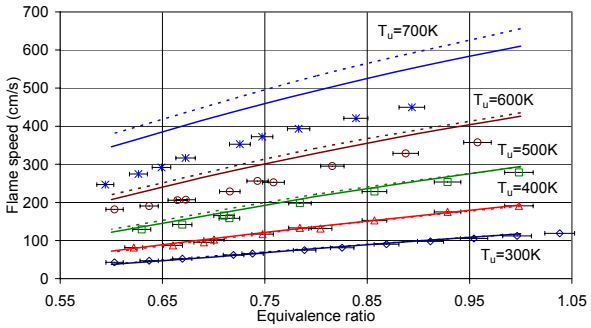

Figure 15. Flame speeds for a 50:50 H_2:CO composition (no dilution) for various preheat temperatures. The curves are results from PREMIX, with GRI-Mech 3.0 (solid lines) and H_2/CO mechanism (dashed lines) of Davis et al.[22]

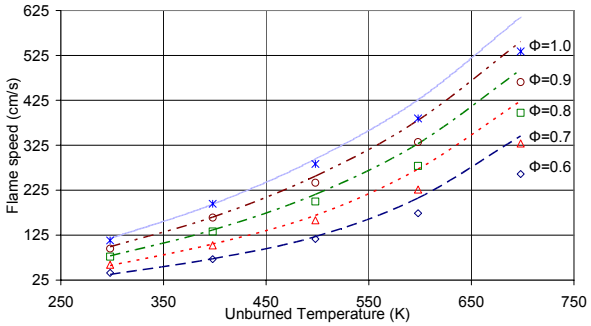

Figure 16. Variation of flame speed with unburned temperature for a H_2:CO 50:50 fuel mixture for various equivalence ratios. The curves are results from PREMIX and GRI-Mech 3.0, and the data points are linearly interpolated at the given ϕ from the data of Figure 15.

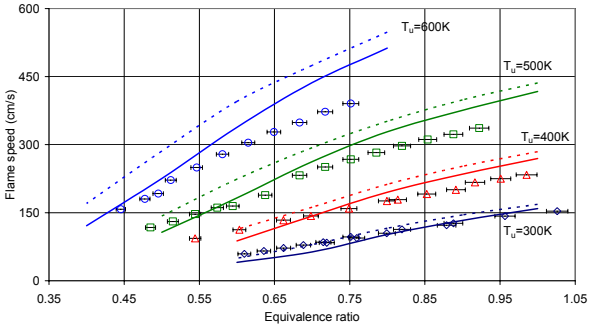

Figure 17. Flame speeds for a 95:5 H_2:CO composition with 20% CO_2 dilution for various preheat temperatures. The curves are results from PREMIX , with GRI-Mech 3.0 (solid lines) and H_2/CO mechanism (dashed lines) of Davis et al.[22]

Preheated flame speed results for the 95:5 H_2:CO composition are shown in Figure 17. For preheated reactants with high H_2 levels, however, the flame speeds (and as a result the jet exit velocities) are extremely high. To reduce the exit velocities and remain laminar, the fuel stream was diluted with 20% CO_2 to reduce the flame speeds. As in the earlier cases, the computed and measured speeds are in fair agreement up to ~400 K. Above this temperature, the discrepancy between the two again increases. Once again, the discrepancy is larger for flame speeds computed with the H_2/CO mechanism. Like the 50:50 case, the computed flame speeds over predict the measured values for all equivalence ratios. For example when the fuel-air mixture is preheated to 600 K, the computed flame speeds over predict the measured value by 10-20% with GRI Mech and by 15-30% with the H_2/CO mechanism.

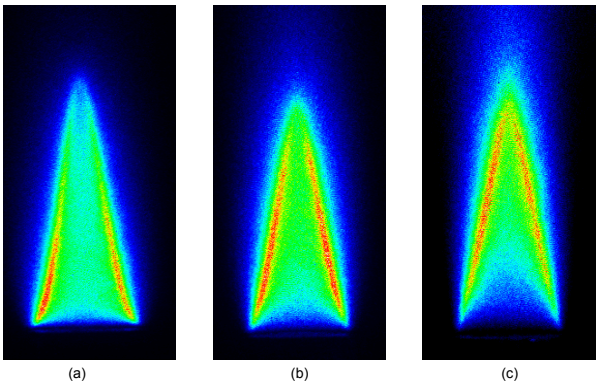

Figure 18. Sample flame images of a 50:50 H_2:CO fuel composition and ϕ=0.78 for unburned temperatures of: (a) 300 K, (b) 500 K, and (c) 700 K.

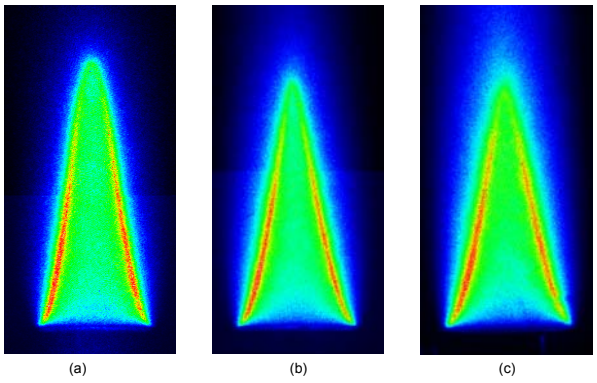

Figure 19. Sample flame images of a 5:95 H_2:CO fuel composition and ϕ=0.81 for unburned temperatures of: (a) 300 K, (b) 500 K, and (c) 700 K.

The difference between the temperature dependence of the measured data and the computed speeds indicates either errors in the temperature dependence of the chemical mechanism or gas properties (e.g., diffusivities) used in the modeling, the increased importance of radiation losses for preheated reactants, or errors in the current measurements. To investigate this last option, Figure 18 shows flame images at three different unburned temperatures for the 50:50 H_2:CO fuel at an

equivalence ratio near 0.78. For the room temperature case (Figure 18a), the image is similar to the previously shown H_2-CO flames (Figure 3), with a bright flame base and an intensity decrease along the flame height. As the unburned temperature increases to 500 K (Figure 18b), the flames becomes more uniform. At the highest temperature (Figure 18c, 700 K), the flame tip intensity increases and the base intensity decreases. (Note, the knife edge was not used in any of these images.) This same behavior is observed for all the equivalence ratios with 50:50 H_2:CO fuel. On the other hand, this behavior is not seen for the 5:95 H_2:CO fuel composition (see Figure 19).

Since the effect is only seen for the higher H_2 concentrations, one explanation is that the increase in flame temperature leads to an increase in thermal OH* emission. The thermal emission would occur in the product gases, and therefore be weighted towards the upper portions of the flame. This would also tend to increase the apparent luminescence zone thickness of the flame, which in turn would increase the measured flame area and reduce the measured flame speed. Thus *it is possible* that the measured flame speeds at high reactant preheat temperature are systematically low, but further work is required to test this theory.

CONCLUSIONS

Laminar flame speeds were measured for syngas fuels over a range of H_2/CO compositions, equivalence ratios, CO_2 dilutions, and reactant preheat temperatures. A laminar premixed jet flame stabilized on the rim of a tube burner was used to measure the laminar flame speed of the syngas mixtures. Average flame speeds were obtained by dividing the volume flow rate of the mixture with the luminous inner cone surface area of the flame. The diagnostic technique was validated with flame speed measurements in CH_4 and H_2/CO flames reported in the literature. The measurements were also compared to numerical calculations of one-dimensional laminar flame speeds obtained using the CHEMKIN PREMIX code and two chemical kinetic mechanisms: GRI Mech 3.0 and a smaller H_2/CO mechanism.

The effect of H_2/CO ratio on flame speed was evaluated in mixtures with H_2 mole fractions ranging from 5 to 95%. Results are in reasonable agreement with the numerical computations and the available data over most of the equivalence ratio range tested. All the measurements are in closer agreement with the flame speeds computations of GRI Mech 3.0 than the H_2/CO mechanism. The impact of CO_2 dilution in H_2/CO mixtures was also measured. As expected, the measured laminar flame speed decreased as the amount of CO_2 dilution was increased at a given equivalence ratio. The measurements and calculations are in good agreement (within 10%) for stoichiometric mixtures and low CO_2 dilutions. However, deviations as large as 30-40% are observed at lean equivalence ratios and high (20% CO_2) dilution levels, with the calculated flame speeds either under predicting or over predicting the measured values depending on the mechanism. While the differences may be related to systematic errors in the current experiment, the data suggest that the current mechanisms should be re-examined for lean, diluted syngas combustion.

The effects of reactant preheat temperature was also evaluated for inlet temperatures up to 700 K. Results show that below about 400 K, the measured flame speeds match the calculated flame speeds within 10%. However, at higher preheat temperatures; the discrepancy between the measurements and the calculations is large, reaching levels of 30% at 700 K. While this may in part be a result of experimental issues, such as increased thermal *OH** emission, it could also indicate the importance of kinetic modeling errors or enhanced radiation effects at high reactant temperatures. Clearly, the effect of preheat temperatures on laminar flame speeds merits further research.

ACKNOWLEDGEMENTS

The authors would like to acknowledge the support of GE Global Research and Development (Dr. Joel Haynes technical monitor) under a subcontract from the U.S. Department of Energy (contract DE-PS26-99FT40578).

REFERENCES

[1]Moliere, M. (2002). "Benefiting from the wide fuel capability of gas turbines: A review of application opportunities." *ASME Paper GT-2002-30017*.

[2]Klimstra, J (1986). "Interchangeability of Gaseous Fuels – The Importance of the Wobbe Index," *SAE Paper 861578*.

[3]Scholte, T. G., and Vaags, P. B. (1959). "Burning velocities of mixtures of hydrogen, carbon monoxide, and methane with air." *Combustion and Flame* **3**, 511-524.

[4]Günther, R., and Janisch, G. (1971). "Messwerte der Flammegeschwindigkeit von gasen und gasmischen." *Chemie-Ing-Techn.* **43**: 975-978.

[5]Strauss, W. A., and Edse, R. (1958). "Burning velocity measurements by the constant-pressure bomb method." *Proceedings of the Combustion Institute* **7**: 377-385.

[6]Yumlu, V. S. (1967). "Prediction of burning velocities of carbon monoxide-hydrogen-air flames." *Combustion and Flame* **11**: 190-194.

[7]Andrews, G. E., and Bradley, D. (1972). "Determination of burning velocities – Critical review." *Combustion and Flame* **18**: 133-153.

[8]Vagelopoulos, C. M., and Egolfopoulos, F. N. (1994). "Laminar flame speeds and extinction strain rates of mixtures of carbon monoxide with hydrogen, methane, and air." *Proceedings of the Combustion Institute* **25**: 1317-1323.

[9]McLean, I. C., Smith, D. B., and Taylor, S. C. (1994). "The use of carbon monoxide/hydrogen burning velocities to examine the rate of the CO + OH reaction." *Proceedings of the Combustion Institute* **25**: 749-757.

[10]Brown, M. J., McLean, I. C., Smith, D. B., and Taylor, S. C. (1996). "Markstein lengths of CO/H_2/air flames, using expanding spherical flames." *Proceedings of the Combustion Institute* **26**: 875-881.

[11]Hassan, M. I., Aung, K. T., and Faeth, G. M. (1996). "Markstein numbers and unstretched laminar burning velocities of wet carbon monoxide flames." *AIAA 96-0912*, *34th Aerospace Sciences Meeting & Exhibit, Reno, NV*.

[12]Hassan, M. I., Aung, K. T., and Faeth, G. M. (1997). "Properties of laminar premixed CO/H_2/air flames at various pressures." *Journal of Propulsion and Power* **13**(2): 239-245.

[13]Ren, J.-Y., Qin, W., Egolfopoulos, F. N., Mak, H., and Tsotsis, T. T. (2001). "Methane reforming and its potential effect on the efficiency and pollutant emissions of lean methane-air combustion." *Chemical Engineering Science* **56**: 1541-1549.

[14]Qin, W., Egolfopoulos, F. N., and Tsotsis, T. T. (2001). "Fundamental and environmental aspects of landfill gas utilization for power generation." *Chemical Engineering Journal* **82**: 157-172.

[15]Kim, T. J., Yetter, R. A., and Dryer, F. L. (1994). "New results on moist CO oxidation: High pressure, high temperature experiments and comprehensive modeling." *Proceedings of the Combustion Institute* **25**: 759-766.

[16]Zhu, D. L., Egolfopoulos, F. N., and Law, C. K. (1988). "Experimental and numerical determination of laminar flame speeds of methane/(Ar, N_2, CO_2) – air mixtures as function of stoichiometry, pressure, and flame temperature." *Proceedings of the Combustion Institute* **22**: 1537-1545.

[17]Lamoureux, N., Djebaili-Chaumeix, N., and Paillard, C. -E. (2003). "Laminar flame velocity determination for H_2-air-He-CO_2 mixtures using the spherical bomb method." *Experimental Thermal and Fluid Science* **27**: 385-393.

[18]Ruan, J., Kobayashi, H., Nioka, T., and Ju, Y. (2001). "Combined effects of nongray radiation and pressure on premixed $CH_4/O_2/CO_2$ flames." *Combustion and Flame* **124**: 225-230.

[19]Ju, Y., Masuya, G., and Ronney, P. D. (1998). "Effects of radiative emission and absorption on the propagation and extinction of premixed gas flames." *Proceedings of the Combustion Institute* **27**: 2619-2626.

[20]Egolfopoulos, F. N., Cho, P., and Law, C. K. (1989). "Laminar flame speeds of methane-air mixtures under reduced and elevated pressures," *Combustion and Flame* **76**: 375-391.

[21]Vagelopoulos, C. M., Egolfopoulos, F. N., and Law, C. K. (1994). "Further considerations on the determination of laminar flame speeds with the counterflow twin-flame technique." *Proceedings of the Combustion Institute* **25**: 1341-1347.

[22]Davis, S. G., Joshi, A. V., Wang, H., and Egolfopoulos, F. (2004). "An optimized kinetic model of H_2/CO combustion." *Proceedings of the Combustion Institute* **30**: 1283-1292.

[23]Mueller, M. A., Yetter, R. A., and Dryer, F. L. (1999). "Flow reactor studies and kinetic modeling of the $H_2/O_2/NO_x$ and $CO/H_2O/O_2/NO_x$ reactions." *International Journal of Chemical Kinetics* **31**: 705-724.